# Quantification of browning kinetics and colour change for quince (Cydonia oblonga Mill.) exposed to atmospheric conditions

Raquel P. F. Guiné[1*], Maria João Barroca[2]

*(1. CI&DETS and Escola Superior Agrária de Viseu, Viseu, Portugal*

*2. Departamento de Engenharia Química e Biológica, ISEC-IPC, Coimbra, Portugal)*

**Abstract:** Because quince is a fruit that shows a very strong tendency for developing an intense browning when exposed to air, even though for short periods of time, the aim of this work was to evaluate the kinetics of colour change for quince exposed to atmospheric air at ambient temperature over a period of 2 hours. The quince was cut into slices that were left exposed to air, and colour measurements were done right after cutting and every 5 min, using a tristimulus colorimeter measuring the CIELab coordinates, L*, a* and b*. The results confirmed that quince suffers a high degree of browning, with total colour difference increasing strongly from 0 to 30 and browning index increasing from 50 to near 140. Furthermore, the major colour changes occurred during the first 30 min of exposure. Different models were tested to fit experimental data and the results showed that the most commonly used models, zero-order and first-order kinetics were totally inadequate in the present case, while the less cited models revealed to be very good at describing the kinetics of colour change for quince: logistic, modified Maskan and exponential rise.

**Keywords:** Quince, total colour difference, browning kinetics, mathematical model.

**Citation:** Guiné, R.P.F., and M. J. Barroca. 2014. Quantification of browning kinetics and colour change for quince (Cydonia oblonga Mill.) exposed to atmospheric conditions. Agric Eng Int: CIGR Journal, 16(4): 285-298.

## 1 Introduction

Quince (*Cydonia oblonga* Mill.) is original from Kydonia on the island of Crete, and has evolved into the fruit we know today, as cultivated in the Mediterranean area, with a shape somewhere between an apple and a pear. In the raw form, the rind is rough and woolly, and the flesh is hard and unpalatable, with an astringent, acidulous taste. Because they are rarely used in the raw form, quinces are commonly transformed into jams and jellies. Once cooked and sweetened, they turn red, taste divine and have a strong pleasant fragrance. Sometimes the quince smells like a tropical fruit. When prepared as jelly, it tastes like a cross between an apple and a pear.

**Received date: 2014-04-09 Accepted date: 2014-11-25**

***Corresponding author: Raquel P. F. Guiné**, ESAV, Quinta da Alagoa, Ranhados, 3500-606 Viseu, Portugal. E-mail: raquelguine@esav.ipv.pt

Colour is one of the most important appearance attributes of food materials, since it strongly influences consumer's acceptability. In fact, undesirable colours like those associated with deterioration or spoilage can eventually lead the consumer to reject the product. In this way it is important for food producers to enhance their products characteristics in order to make them appealing for consumers (Maskan, 2001). The colour of food products may be affected in a high extent by processing operations, in particular thermal processing. However, some degradation also occurs during transportation and storage of foods. Among the alterations that can occur are those resulting from pigment degradation, in particular chlorophyll and carotenoids (lycopene, xanthophylls, etc.), as well as browning reactions such as Maillard condensation of hexoses and amino components, enzymatic browning and oxidation of ascorbic acid (Maskan, 2001, 2006; Suh

et al., 2003). Besides these, other factors that affect colour include some fruit characteristics like pH or acidity, fruit cultivar and heavy metal contaminations, and also processing conditions such as temperature and processing time, or even the presence of oxygen (Iglesias, 2012; Nordey, 2014; Nuncio-Jáuregui, 2014).

Because colour is so important for the access of food products quality, it has been the object of study by many researchers. Examples are the evaluation of colour changes during processing of pomegranate juice concentrate (Maskan, 2006), colour change of tofu during deep-fat frying (Baik and Mittal, 2003), colour change for microwave and air drying of kiwis (Maskan, 2001), degradation of green colour in spinach (Nisha et al., 2004), colour change in watercress for heat and thermosonication treatments (Cruz et al., 2007), colour changes during dehydration of carrots (Koca et al., 2007), variation of colour of bananas during drying (Chua et al., 2001). Apart from processing, also the degradation of colour during storage or maturation is important and was studied for example by Chen and Ramaswamy (2002) for the ripening of bananas. Furthermore, Quevedo et al. (2009) quantified the enzymatic browning in pear slices exposed to atmospheric air at 10℃ for 140 min.

The instrumental measurement of colour is usually based on the principle that a colour can be mathematically described as a combination of the three primary colour intensities. In this way, tristimulus colorimetry has been widely accepted as a rapid and simple instrumental method for measuring the colour of food products (Nisha et al., 2004; Corzo et al., 2006). CIELab Cartesian coordinates (L*, a*, b*) have been extensively used to access colour in many foods, like fruits and vegetables, and has proved valuable in evaluating colour degradation and providing useful information for quality control in foods (Maskan, 2001). There are other parameters derived from Hunter L*, a*, b* coordinates, such as the total colour difference (Delta-E), which aims at quantifying the overall colour difference between a sample and a reference material. Furthermore, the Cartesian coordinates can be used to calculate the cylindrical coordinates: the saturation index or chroma and the Hue angle. While chroma indicates colour saturation and is proportional to the intensity, the Hue angle is used to characterise the colour of foods (Maskan, 2001). In the CIELhc system a circle of 360 ° includes four principal hues: red, yellow, green and blue, while in the Munsell system each circle is divided into five principal hues: red, yellow, green, blue, and purple, along with five intermediate hues halfway between adjacent principal hues.

Data about the kinetics of change in quality attributes in foods, like for example colour, including order of reaction, reaction rate constants and temperature dependence, provide valuable information for understanding and predicting changes that occur during processing and storage, and therefore are important for maximizing quality and minimizing losses (Kumar et al., 2006).

As previously stated, many studies can be found in scientific literature about the kinetics of colour change during processing of different food products, and also some about storage. However, studies about the kinetics of degradation of colour of quince just by exposure to the atmospheric air are lacking, and this is a product that is very susceptible to browning in a very short time, thus sometimes limiting its usage. In this way, the present study was undertaken to investigate the variation along time of measurable colour using Hunter colour space L*a*b* during exposure of quince to atmospheric conditions, and also to test different kinetic models to verify which of them apply best to the experimental data.

## 2 Materials and methods

### 2.1 Sampling

The samples of quince (*Cydonia oblonga* Mill.) cultivar ‘Gamboa’ were cut into slices (thickness of 1 cm) for the colour evaluations. Then, the same slices were left exposed to atmospheric conditions in the laboratory at a temperature around 18℃ and a relative humidity in the range 20%-30%. The laboratory was well illuminated,

with some natural illumination coming from the windows and also the artificial light from the lamps. Along the exposure colour measurements were made every 5 min, always on the same samples, stopping after two hours.

**2.2 Colour measurements**

The colour was measured using a handheld tristimulus colorimeter (Chroma Meter - CR-400, Konica Minolta). A CIE standard illuminant D65 was used for calibration and the colour coordinates L*a*b* of the CIELab colour space were determined. From the Cartesian coordinates (L*a*b*) the total colour difference (Delta-E) was calculated by Equation (1) (Chen and Ramaswamy, 2002):

$$\text{Delta - E} = \sqrt{(L^*_0 - L^*)^2 + (a^*_0 - a^*)^2 + (b^*_0 - b^*)^2} \quad (1)$$

having the freshly cut product as reference, with coordinates $L^*_0$, $a^*_0$, $b^*_0$. Delta-E is a colorimetric parameter extensively used to characterize variation in colour and a larger Delta-E means greater deviation from the initial colour of the reference material.

The Cartesian colour coordinates were then used to calculate the cylindrical coordinates, chroma and hue angle, by the following equations (Maskan, 2001).

$$\text{Chroma} = \sqrt{a^{*2} + b^{*2}} \quad (2)$$

$$\text{Hue}\ (^o) = \tan^{-1}\left(\frac{b^*}{a^*}\right) \quad (3)$$

Chroma, sometimes also called saturation, is the purity of a colour, measuring how intense it is: high chroma colours look rich and full while low chroma colours look dull and grayish. Hue is the actual colour of an object. An angle of 0° or 360° represents red Hue, while angles of 90°, 180° and 270° represent yellow, green and blue Hue, respectively (Maskan, 2001).

According to Maskan (2001) the browning index (BI) can be calculated from the Cartesian colour coordinates by the following Equation (4):

$$BI = \frac{[100\,(x - 0.31)]}{0.17} \quad (4)$$

where

$$x = \frac{(a^* + 1.75\,L^*)}{(5.645\,L^* + a^* - 3.012\,b^*)} \quad (5)$$

For the colour determinations ten samples were analysed for each state (fresh and different dryings) and the mean values and standard deviations were calculated for each set.

**2.3 Modelling the kinetics of colour change and browning**

The application of kinetic models to describe the change of a certain property of food during processing or storage has been studied by many authors (Baik and Mittal, 2003; Corzo et al., 2006; Demir et al., 2002; Maskan, 2006; Nisha et al., 2004). In general, the rate of change of a certain property represented by P can be given by the following Equation (6):

$$\frac{dP}{dt} = -k(P)^n \quad (6)$$

where P is the value of the property at question in time t, k stands for the rate constant and n is the order of reaction (Broyart et al., 1998; Chen and Ramaswamy, 2002; Lau et al., 2000). Integration of Equation (6) can lead to several kinetic models, like zero-order, first-order or fractional conversion, represented respectively by Equations (7), (8) and (9).

$$P = P_0 \pm k_0\,t \quad (7)$$

$$P = P_0\exp(\pm k_1\,t) \quad (8)$$

$$\frac{(P - P_e)}{(P_0 - P_e)} = \exp(\pm k_2\,t) \quad (9)$$

In the above equations $P_0$ represents the initial value of the property while $P_e$ is the final equilibrium value, and the signs (+) or (-) indicate increase or degradation of the property P, respectively (Chen and Ramaswamy, 2002; Maskan, 2006). The zero-order and first-order models are among those most frequently cited in literature (Ávila and Silva, 1999; Chutintrasri and Noomhorm, 2007; Cruz et al., 2007; Ilo and Berghofer, 1999; Koca et al. 2007; Ochoa et al., 2001; Topuz, 2008).

Another model cited in literature to describe the kinetics of change of a certain attribute is the logistic model reported by Chen and Ramaswamy (2002) as:

$$P = P_0 + \frac{P_e}{1 + \exp\left[\pm k_3 (t - t_0)\right]} \quad (10)$$

where $t_0$ is the half-life time, i.e., the time at which the value of the property P increases/decreases to half/double of the value.

Quevedo et al. (2009) reported a power-law model for describing the kinetics of enzymatic browning in pear slices, similar to Equation (8), but in which the order of reaction is not fixed:

$$\frac{P}{P_0} = \exp(\pm k_4 t^n) \quad (11)$$

where $P/P_0$ is the conversion fraction of one property with respect to the initial value, n is the shape factor and $k_4$ is the rate parameter. When $k_4$ is positive the kinetics is an exponential growth and when it is negative it is an exponential decay.

Maskan (2006) used a combined kinetic model for the colour degradation kinetics of pomegranate juice, which combines the zero-order and first-order kinetic constants, respectively $k_0$ and $k_1$ in Equations (7) and (8). The model in Equation (12) is similar to that referred by Maskan (2006). This model, named modified Maskan, was used to fit the experimental data for total colour difference (Delta-E) and browning index (BI), because these two properties are those that better show the colour evolution along time.

$$P = \frac{k_0}{k_1} - \left[\frac{k_0}{k_1} - P_0\right] \exp(\pm k_1 * a * t) \quad (12)$$

Furthermore, the variables Delta-E and BI were also fitted to a different model, an exponential rise to maximum function of the type.

$$P = P_0 + a\left[1 - \exp(-k_5 t)\right] \quad (13)$$

For the fittings the software SigmaPlot V8.0 (SPSS, Inc.) was used.

**2.4 Statistical analysis**

The goodness of the fits was evaluated firstly considering the values of the coefficient of determination ($R^2$) and also on different statistical evaluations (Mean absolute error – MAE, Root mean square error – RMSE, Standard error – SE, Sum of square errors – SSE, Chi square – CS and Relative percent deviation - RPD , as described by standard equations as described below (Al-Harahsheh et al., 2009; Lee and Kim, 2009; Roberts et al., 2008; Tripathy and Kumar, 2009; Vega-Gálvez et al., 2009).

Mean absolute error:

$$MAE = \frac{1}{N}\sum_{i=1}^{N}\left|V_{exp,i} - V_{pred,i}\right| \quad (14)$$

Root mean square error:

$$RMSE = \sqrt{\frac{1}{N}\sum_{i=1}^{N}\left(V_{exp,i} - V_{pred,i}\right)^2} \quad (15)$$

Standard error:

$$SE = \frac{\sqrt{\sum_{i=1}^{N}\left(V_{exp,i} - V_{pred,i}\right)^2}}{N-1} \quad (16)$$

Sum of square errors:

$$SSE = \frac{1}{N}\sum_{i=1}^{N}\left(V_{exp,i} - V_{pred,i}\right)^2 \quad (17)$$

Chi square:

$$CS = \frac{1}{N - n_p}\sum_{i=1}^{N}\left(V_{exp,i} - V_{pred,i}\right)^2 \quad (18)$$

Relative percent deviation:

$$RPD = \frac{100}{N}\sum_{i=1}^{N}\frac{\left|V_{exp,i} - V_{pred,i}\right|}{V_{exp,i}} \quad (19)$$

In these equations N stands for the number of observations and $n_p$ for the number of parameters, while $V_{exp,i}$ and $V_{pred,i}$ are the experimental and predicted values for the dependent variable at any observation i. A better quality of the fit is obtained with higher values of $R^2$, and values of CS and RMSE approaching zero indicate that the prediction is closer to the experimental data (Lee and Kim, 2009; Roberts et al., 2008). On the other hand, RMSE and CS aim at comparing the differences between the experimental and predicted values of the dependent variable, while the relative percent deviation compares

the absolute differences between them. Therefore, a good fit will be obtained if the value of RPD is under 10% (Roberts et al., 2008).

## 3 Results and discussion

### 3.1 Colour evaluations

Figures 1 to 3 show the variations along time of the experimental values measured for the Cartesian colour coordinates: L*, a* and b*. In the graphs the mean values calculated from ten measurements at each time instant are presented, together with the corresponding standard deviation. The values found for the Cartesian coordinates in the freshly cut quince were respectively 78.02(±0.86), -1.27(±0.23) and 31.75(±1.68) for L*, a* and b*. These values indicate that the quince pulp is clear, having a high value of the coordinate lightness or brightness (L*), just slightly green, with a negative value of a*, although very close to zero, and very yellow, as seen by the positive and high value of b*. Furthermore, it is possible to see that the pulp is quite homogeneous in colour when the measurements are made immediately after cutting, given the very small values of the standard deviations for all coordinates. By observing Figures 1 2 and 3, is possible to see that for the colour measurements made at 5 min and thereafter, the standard deviations are higher, what is natural, since the browning reactions do not occur all exactly at the same rate in all the exposed quince, thus giving place to a spotted surface, with some darker zones and some others a little less dark.

Figure 1 shows the variation along the two hours of exposure of the coordinate L* and we can see from the graph that lightness diminishes from a value near 80 to around 50, indicating a very important degree of darkening. Furthermore, the rate of changing is much higher in the initial states of exposure as compared to the final periods, where a stabilization is observed. In fact, 75% of the total change in L* occurred during the first 30 min, while during the other hour and a half the variation was much smaller. Maskan (2001) for different drying treatments in kiwi also reported a decrease in L coordinate from around 47 to 40, 34 or 30 depending on treatment: microwave, hot air or combined microwave with hot air, respectively. Baik and Mittal (2003) observed a decrease in L value from around 85 to 70 for the processing of tofu. Ávila and Silva (1999) for the colour degradation in spinach during thermal treatment also observed a decrease in L coordinate, indicative of darkening.

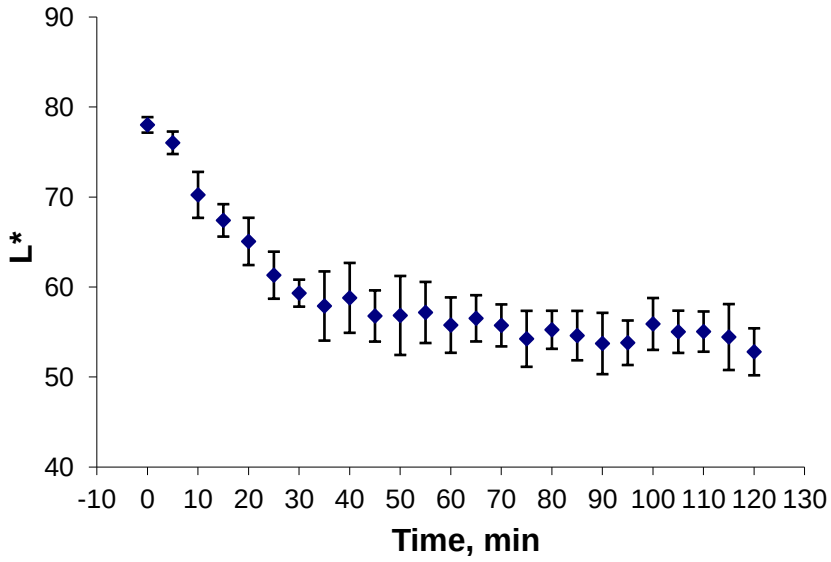


Figure 1 Variation along time of colour coordinate L*

Regarding the colour coordinate a*, presented in Figure 2, the initial value, as previously stated, is slightly negative and negative values of a* indicate green colour. However, this rapidly changes to positive, the red zone, with the medium value at 5 min already positive and equal to 1.53. As to variation of this colour coordinate, in the two hours of exposure the total variation goes from -1.27 to 17.98, corresponding to an important intensification of the red colour. Once again the first half hour of exposure was the most critical, corresponding to 83% of the increase in a*. Cruz et al. (2007) for the heat and thermosonication treatment of watercress observed an important increase in the colour coordinate a.

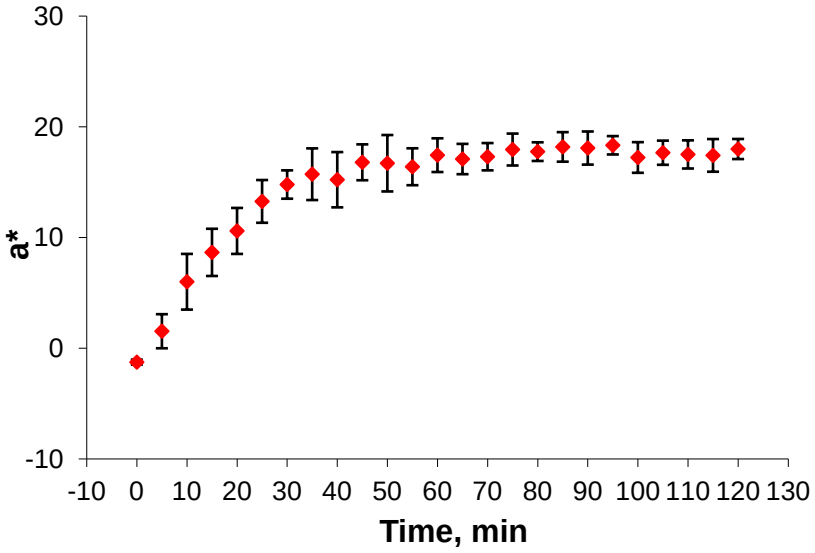


Figure 2 Variation along time of colour coordinate a*

With respect to the other opposing colour coordinate, b*, (Figure 3) this suffers an increase from around 32 to 38, being this the coordinate that changed less of all three. In fact, the initial value of b* was already quite high, corresponding to an intense yellow, and the browning only intensified a little the yellow colour. Also in this case the change in the first 30 min was pivotal, corresponding in the present case to near 100% of the total change in b*, since after this time a stabilization was achieved, with the values of b* keeping only oscillating around the final value. Hence, the value of b* increased along exposure time, which is in accordance with the finding of Chen and Ramaswamy (2002), who observed an increase in colour coordinate b* for bananas during ripening for storage at different temperatures.

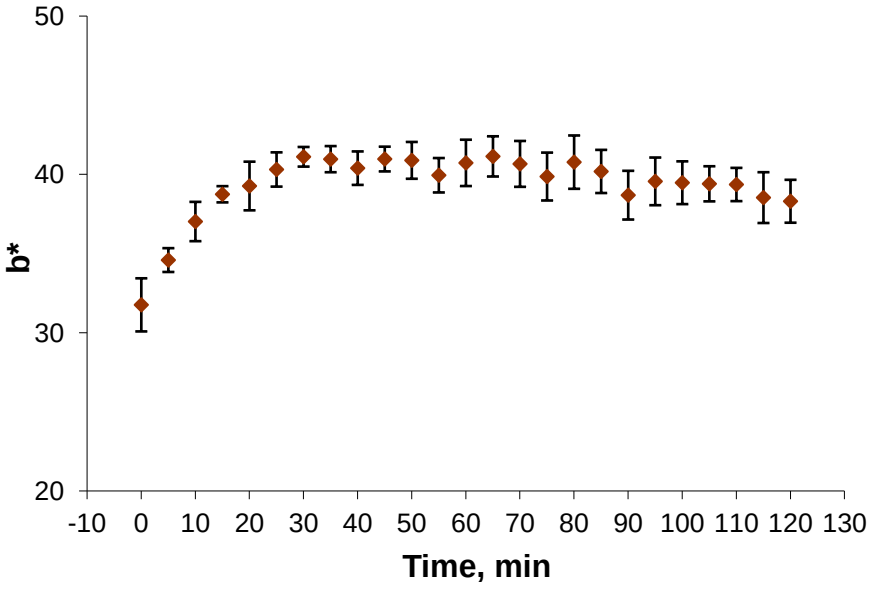


Figure 3 Variation along time of colour coordinate b*

Figure 4(a) shows the variations along exposure time of the cylindrical coordinates, chroma and hue angle, as calculated by Equations (2) and (3), from the corresponding values of the Cartesian coordinates for every time t. Chroma, which indicates colour saturation, increases along time from about 32 to 42, thus indicating an intensification of colour. The hue angle decreased from approximately 90 º to 65 º, thus moving from the fully yellow colour to the red zone, although staying far from the fully red (0 º). Maskan (2001) observed a change in the values of chroma and hue for kiwifruit for microwave drying: chroma diminished from 18.04 to 15.93 and hue angle decreased from 97.16 to 74.27, for treatments during 25 min. For hot air drying chroma diminished from 17.99 to 16.22 and hue from 97.02 to 80.42 for 330 min of treatment and for the combined heat treatment chroma changed to 15.54 and hue to 65.47 for 139 min treatment.

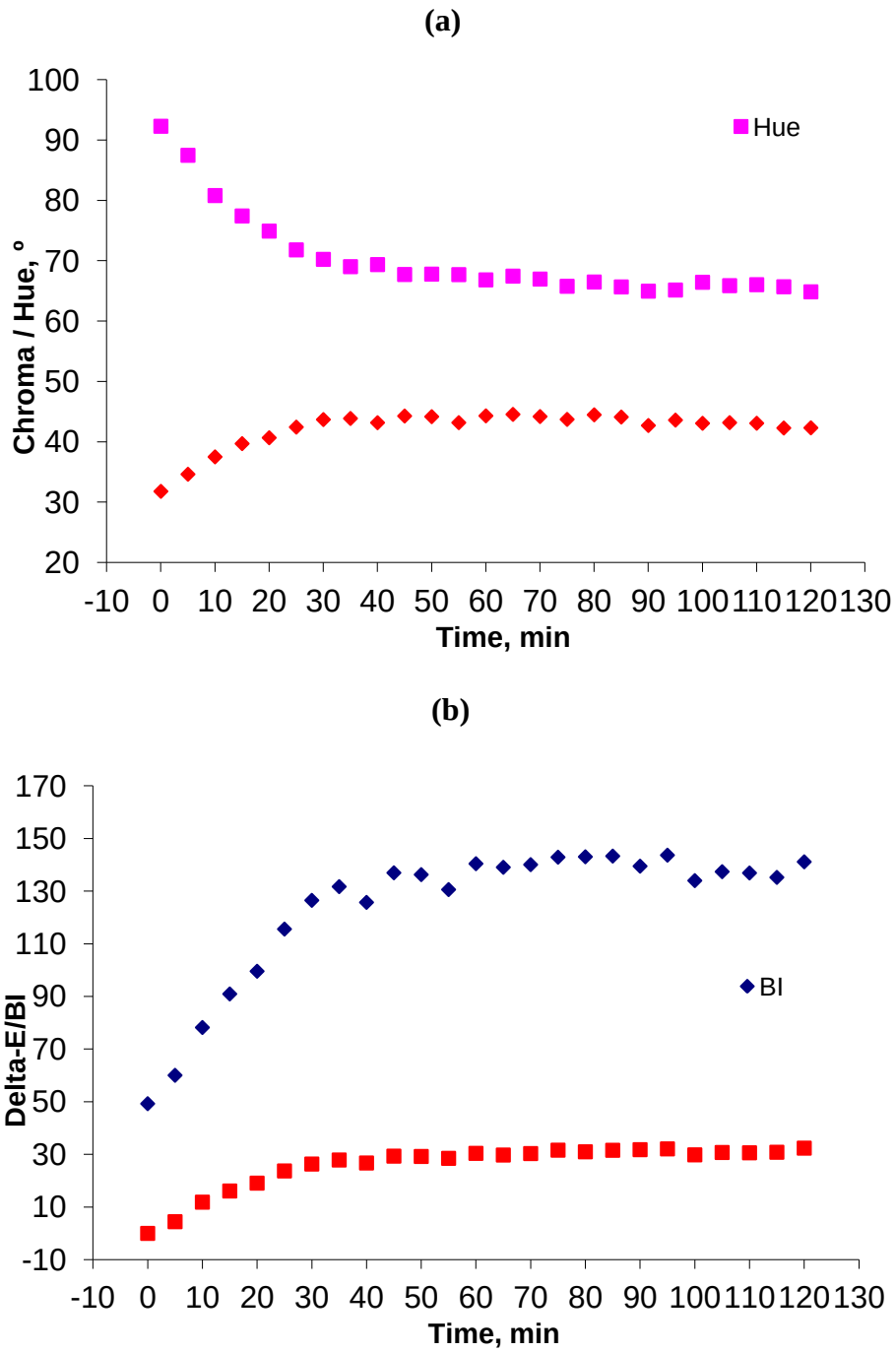


Figure 4 Variation along time of the cylindrical coordinates chroma and hue angle (a), total colour difference and browning index (b)

Total colour difference in Equation (1) evaluates the overall deviation of a colour from that considered reference, which in the present case was the colour of the quince right after cutting. The variation of total colour difference is shown in Figure 4(b) increasing very rapidly in the first 30 min and showing stabilization thereafter. The Delta-E increased from zero to around 30, thus indicating an intense colour variation, particularly at the early stages of exposure. Baik and Mittal (2003) observed an increase in Delta-E to a final value of 20 for the processing of tofu. Ávila and Silva (1999) for the thermal treatment of spinach reported an increase in Delta-E which varied according to process conditions, up to a value of 16. These values on increase in delta e reported in literature are lower than what we found on this work,

which might be explained by the high susceptibility of quince for darkening when exposed to air.

The variation of the Browning index, as defined by Equation (4) shows a similar trend to that observed for delta-E, and also increases quite significantly from an initial value around 50 to a final value of near 140. Maskan (2001) at evaluating the colour change of kiwi during microwave drying observed an increase in BI from 42.15 to 78.93 over 25 min. For the hot air drying the increase in BI was from 42.11 to 54.38 in 330 min and for combined heat treatment BI increased to 67.40 in 139 min. Once again the values for increase in BI reported in literature were not so high as for quince, which shows a very intense browning.

**3.2 Kinetics of colour change**

Tables 1 and 2 show the results of the fittings made to the different colour parameters evaluated, the Cartesian coordinates (L*, a*, b*), the cylindrical coordinates (Chroma, Hue), the total colour difference and browning index, by applying the models in Equations (7) to (11), those most frequently cited in literature to describe the kinetics of colour change, particularly the zero-order and first-order kinetics. (Chen and Ramaswamy, 2002; Chutintrasri and Noomhorm, 2007; Corzo et al., 2006; Koca et al., 2007; Kumar et al., 2006; Nisha et al., 2004) Although in the graphs presented with the variations of the colour variables along time, this was expressed in min, so as easily show the time evolution of these variables (Figures 1 to 4), for the evaluation of the kinetics of colour change the time data was used in seconds, so as to estimate the values of the kinetics constants in $sec^{-1}$, for being the International System unit for time, and the corresponding parameters obtained are all in the same system.

In Tables 1 and 2 the estimated values of the different parameters in each model are presented, together with the values of the coefficient of determination, $R^2$, which characterizes each estimation. The results in Tables 1 and 2 show that in the present case the zero-order model is not at all adequate for describing the kinetics of colour change, since the values of $R^2$ are too low, being the highest obtained for the fit of L*, but still not acceptable, 0.6783. On the other hand, also the first-order kinetics is not admissible in the present case, for the same reasons pointed out previously, i.e., too low values of the determination coefficients, ranging from 0.1096 to 0.7135. As to the fractional model, it seems to fit with some accuracy the experimental data for L* ($R^2$ = 0.9821) or Hue ($R^2$ = 0.9927), but in other cases it revealed to be fairly inadequate, like for b* ($R^2$ = 0.1089). The logistic model showed to be very proper to fit the kinetics of colour change in the present cases, and the values obtained for the coefficient of determination are relatively reasonable for all variables, ranging from 0.8615 in the case of b* to 0.9936 for a*. The power-law model, showed in some cases a relatively good fitting, like for L* ($R^2$=0.9047), and in some other cases a bad fitting, like for b* ($R^2$=0.6604). Therefore, from the 5 kinetic models tested in this phase, the logistic was the one that showed a better adequacy for describing the kinetics of colour change, with a good representation for all variables colour tested.

Since the majority of the works about kinetics of colour change used zero-order or first-order kinetics, and in the present case these models revealed to be completely inadequate for describing the kinetics of colour change, the values of the kinetic constants are not comparable with some other reported in literature. Even for other models, less frequently cited, the products and conditions are not the same as in the present study, making it difficult any type of comparison. However, it is worth mention some of those studies. Ávila and Silva (1999) studied the kinetics of colour degradation in peach pure during thermal treatment, and used the fractional conversion equation for modelling. They found values of the kinetic constant of 0.0029, 0.0040, 0.0300 and 0.0085, min respectively for the colour variables L, a, b

**Table 1 Fitting of the experimental data with models from Equations (7) to (9)**

| | L* | a* | b* | Delta-E | Chroma | Hue | BI |
|---|---|---|---|---|---|---|---|
| Zero-order: Equation (7) | | | | | | | |
| $P_0$ | 68.3762 | 7.7547 | 38.1111 | 14.5841 | 39.1707 | 79.4354 | 90.2921 |
| $k_0$ ($s^{-1}$) | -2.57e-3 | 1.89e-3 | 3.29e-4 | 3.13e-3 | 8.34e-4 | -2.57e-3 | 9.35e-3 |
| $R^2$ | 0.6783 | 0.6048 | 0.1137 | 0.6178 | 0.3372 | 0.62787 | 0.5907 |
| RMSE | 1.2845 | 3.0428 | 4.0428 | 2.6482 | 5.0647 | 4.0674 | 5.0974 |
| RPD | 9.4187 | 11.4197 | 15.7164 | 10.5412 | 13.0945 | 9.8412 | 11.0648 |
| First-order: Equation (8) | | | | | | | |
| $P_0$ | 69.3551 | 9.6027 | 38.1643 | 17.4462 | 39.3689 | 80.2969 | 96.2077 |
| $k_1$ ($s^{-1}$) | -4.58e-5 | 1.09e-4 | 8.06e-6 | 1.04e-4 | 1.89e-5 | -3.84e-5 | 6.77e-5 |
| $R^2$ | 0.7135 | 0.5128 | 0.1096 | 0.5296 | 0.3221 | 0.6580 | 0.5308 |
| RMSE | 2.0764 | 3.6715 | 5.7054 | 3.0705 | 6.7150 | 2.0714 | 3.7015 |
| RPD | 8.7165 | 10.9451 | 16.0751 | 9.7164 | 14.8154 | 8.9045 | 11.0974 |
| Fractional: Equation (9) | | | | | | | |
| $P_0$ | 79.3932 | 7.8624 | 38.1675 | 14.6784 | 39.2134 | 92.7958 | 90.5419 |
| $P_e$ | 54.2177 | -315.36 | -2.8927 | -938.78 | -167.30 | 65.7179 | -3302.3 |
| $k_2$ ($s^{-1}$) | -7.66e-4 | 5.16e-6 | 7.12e-6 | 3.20e-6 | 3.93e-6 | -9.26e-4 | 2.69e-6 |
| $R^2$ | 0.9821 | 0.5833 | 0.1089 | 0.6150 | 0.3341 | 0.9927 | 0.5882 |
| RMSE | 1.9457 | 5.7415 | 6.7154 | 3.4152 | 5.1247 | 1.1045 | 4.5127 |
| RPD | 3.7415 | 11.8450 | 16.7154 | 11.0451 | 13.8041 | 2.7154 | 12.0741 |

**Table 2 Fitting of the experimental data with models from Equations (10) and (11)**

| | L* | a* | b* | Delta-E | Chroma | Hue | BI |
|---|---|---|---|---|---|---|---|
| Logistic: Equation (10) | | | | | | | |
| $U_0$ | 54.6055 | -21.421 | 29.1377 | -36.138 | 27.3189 | 290.72 | 15.2884 |
| $U_e$ | 58.1742 | 39.1257 | 10.9047 | 67.1939 | 16.27523 | -1020.1 | 124.178 |
| $t_0$ | -325.23 | -25.239 | 317.35 | -96.508 | 402.94 | -2328.8 | 626.87 |
| $k_3$ ($s^{-1}$) | 1.04e-3 | -1.29e-3 | -3.55e-3 | -1.25e-3 | -2.34e-3 | 65.781 | -1.58e-3 |
| $R^2$ | 0.9837 | 0.9936 | 0.8615 | 0.9906 | 0.9573 | 0.9926 | 0.9839 |
| RMSE | 2.7154 | 1.0412 | 2.9154 | 0.9457 | 2.9945 | 0.8425 | 1.9427 |
| RPD | 3.7465 | 2.9145 | 4.8154 | 1.9485 | 5.4151 | 1.9451 | 2.9847 |
| Power-law: Equation (11) | | | | | | | |
| $P_0$ | 80.3103 | 4.13e-7 | 31.6685 | 8.36e-8 | 31.4586 | 94.0408 | 46.8036 |
| n | -0.0190 | 13.3500 | 0.1049 | 16.0844 | 0.0735 | -0.0283 | 0.1351 |
| $k_4$ ($s^{-1}$) | 0.3510 | 0.0326 | 0.0941 | 0.0242 | 0.1758 | 0.2963 | 0.2459 |
| $R^2$ | 0.9047 | 0.7377 | 0.6604 | 0.7813 | 0.7743 | 0.9152 | 0.8614 |
| RMSE | 2.7145 | 6.7154 | 5.7124 | 6.7154 | 5.7154 | 2.0487 | 4.0175 |
| RPD | 3.8154 | 8.7164 | 9.7154 | 8.7154 | 7.9425 | 3.8146 | 6.7154 |

and Delta-E. Quevedo et al. (2009) studied the kinetics of enzymatic browning for pear slices left at room temperature (10℃) for 140 min, by means of the power-law model. They found for the variation of L* along time that the kinetic constant varied from -0.002 to -0.007 $min^{-1}$, according to pear cultivar, and n varied from 0.56 to 0.68. Ochoa et al. (2001) also used the power-law model for quantifying the kinetics of colour change of different preserves by the effect of light and room temperature, and reported values of the kinetic constant varying from 0.0220 to 0.0550 $days^{-1}$. Topuz (2008) for the colour degradation kinetics of paprika

modelled by the fractional conventional equation, found values of the constant between 108.7 and 124.8 $h^{-1}$ for colour parameter L, between 99.0 and 109.0 $h^{-1}$ for a, between 97.1 and 108.5 $h^{-1}$ for b, and finally between 99.9 and 110.7 $h^{-1}$ for delta-E, and depending on the water activity level. These valued reported in literature are a little higher than those found on the present work and shown in Table 1.

In a second phase, the most important variables that account for the colour change, the total colour change and the browning index, were used to test three kinetic models: the one that revealed to be the best in the previous phase of evaluation – the logistic model, together with the modified Maskan model from Equation (12) and still another model, an exponential raise function as expressed by Equation (13). In this second attempt to compare the different kinetic models, and since the number of variables to fit was diminished from seven to two, and the number of models was decreased from five to three, a more detailed statistical analysis was done for the evaluation and comparison of models. Tables 3 and 4 s

res

corresponding values of the different statistical variables estimated. As to the variable Delta-E, the results in Table 3 shows that the logistic and the exponential rise models are the ones that present the lower values of relative percent deviation (RPD), 3.463 and 4.181, respectively. However even for the modified Maskan model the value of RPD is acceptable, 7.621, because any value under 10% means that the fit is good (Roberts et al., 2008). In all cases the values of the mean absolute error (MAE) are low and so are those of the standard error (SE) and sum of square errors (SSE). As to the values of the root mean square error (RMSE) and chi square (CS) they are also small in all cases, thus indicating a good fit, particularly for model logistic and exponential rise. Values of CS and RMSE close to zero indicate that the prediction given by the model is very close to the experimental data. Figure 5 shows the experimental data for Delta-E together with the fittings obtained with the three models, and the graph shows a good adequacy of all models, including the modified Maskan, whose statistical variables were those that differed a little more

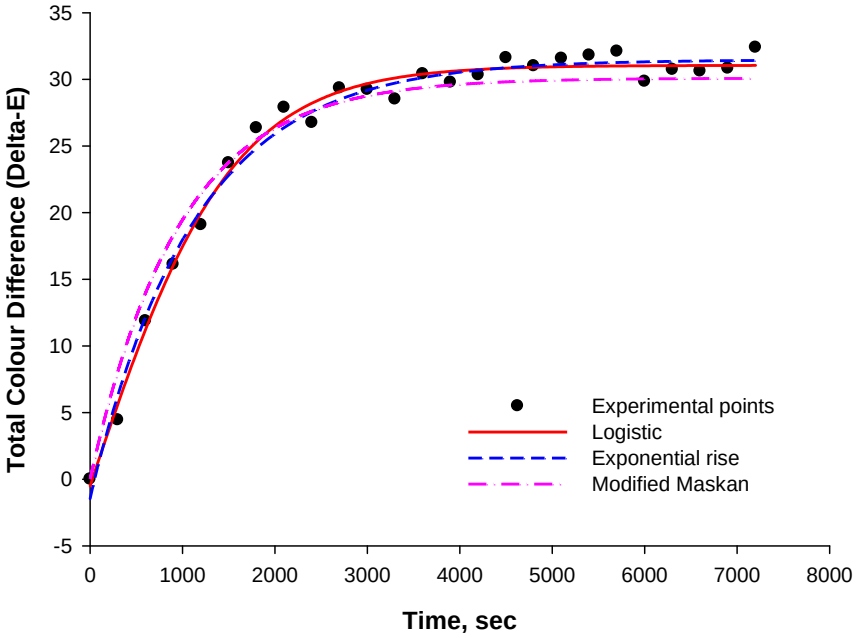


Figure 5 Experimental variation of Delta-E along time and fittings with the more adequate models

**Table 3 Fitting of the experimental data of total colour difference (Delta-E) with models from Equations (10), (12) and (13) and statistical analysis**

| Parameters | | | | | |
|---|---|---|---|---|---|
| **Logistic** Equation (10) | | **Modified Maskan** Equation (12) | | **Exponential rise** Equation (13) | |
| $P_0$ | -3.6138 | $P_0$ | 0.000 | $P_0$ | -1.463 |
| $P_e$ | 6.7194 | **a** | 10.000 | **a** | 3.2938 |
| $t_0$ | -9.6508 | $k_0$ ($s^{-1}$) | 3.13e-3 | $k_5$ ($s^{-1}$) | 8.89e-4 |
| $k_3$ ($s^{-1}$) | -1.25e-3 | $k_1$ ($s^{-1}$) | 1.04e-4 | | |
| **Statistics** | | | | | |
| **N** | 25 | **N** | 25 | **N** | 25 |
| $n_p$ | 4 | $n_p$ | 4 | $n_p$ | 3 |
| **MAE** | 0.713 | **MAE** | 1.208 | **MAE** | 0.817 |
| **RMSE** | 0.835 | **RMSE** | 1.491 | **RMSE** | 0.941 |
| **SE** | 0.174 | **SE** | 0.311 | **SE** | 0.196 |
| **SSE** | 0.697 | **SSE** | 2.223 | **SSE** | 0.886 |
| **CS** | 0.829 | **CS** | 2.646 | **CS** | 1.007 |
| **RPD** | 3.463 | **RPD** | 7.621 | **RPD** | 4.181 |

**Table 4 Fitting of the experimental data of browning index (BI) with models from Equations (10), (12) and (13) and statistical analysis**

| Parameters | | | | | |
|---|---|---|---|---|---|
| **Logistic** Equation (10) | | **Modified Maskan** Equation (12) | | **Exponential rise** Equation (13) | |
| $P_0$ | 15.2884 | $P_0$ | 49.277 | $P_0$ | 42.427 |
| $P_e$ | 124.178 | **a** | 13.000 | **a** | 99.064 |
| $t_0$ | 626.87 | $k_0$ ($s^{-1}$) | 9.35e-3 | $k_5$ ($s^{-1}$) | 8.52e-4 |
| $k_3$ ($s^{-1}$) | -1.58e-3 | $k_1$ ($s^{-1}$) | 6.77e-5 | | |
| **Statistics** | | | | | |
| **N** | 25 | **N** | 25 | **N** | 25 |
| $n_p$ | 4 | $n_p$ | 4 | $n_p$ | 3 |
| **MAE** | 2.723 | **MAE** | 4.618 | **MAE** | 3.906 |
| **RMSE** | 3.334 | **RMSE** | 5.318 | **RMSE** | 4.357 |
| **SE** | 0.695 | **SE** | 1.108 | **SE** | 0.908 |
| **SSE** | 11.112 | **SSE** | 28.282 | **SSE** | 18.981 |
| **CS** | 13.229 | **CS** | 33.670 | **CS** | 21.569 |
| **RPD** | 2.195 | **RPD** | 4.087 | **RPD** | 3.635 |

Table 4 shows the results of the fitting to the data of BI with the same three models as used for variable Delta-E, and the results are somehow similar. In fact, also in this case the best model, as indicated by the statistical variables considered, is the logistic, followed by the exponential rise and finally the modified Maskan. However, in all cases the values of the RPD are under 10%, thus indicating that the fits are adequate to describe the variation of BI along time. However, in this case the values of the CS are quite higher when compared to those for Delta-E, although the values of RMSE are still low. Figure 6 shows the experimental points of BI together with the curves representing the different fits, and also in this case a good representation was achieved.

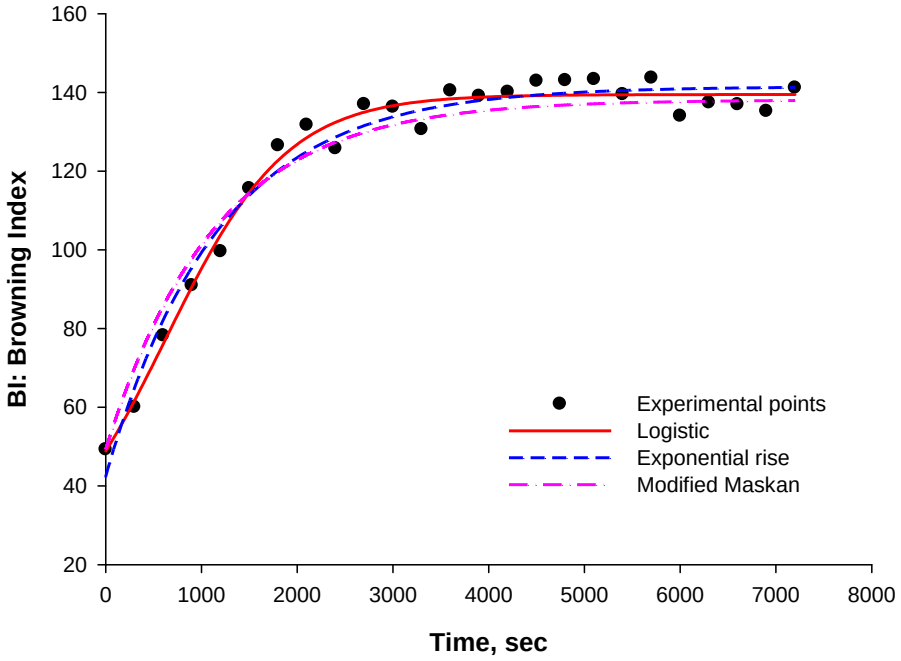


Figure 6 Experimental variation of BI along time and fittings with the more adequate models

It is however very interesting to notice that although the zero-order and first order-kinetics revealed totally inadequate to describe the kinetics of colour change for these two variables considered (Delta-E and BI), and therefore the values of $k_0$ and $k_1$ alone do not have any meaning in kinetic terms, the truth is that the modified Maskan model, which uses a combination of these two parameters revealed to quite fairly predict the kinetics of change for these variables.

## 4 Conclusions

From the results obtained, it was possible to conclude that quince is very sensitive to air exposure, even if just at atmospheric air, showing important variations in brightness, diminishing from near 80 to around 60, thus indicating a strong darkening, as well as significant increases in both coordinates a* and b*, of about 20 and 10 points respectively. Furthermore, a decrease in Hue was also observed together with an increase in chroma. As to the overall colour change indicators Delta-E and BI, these increase quite considerably, confirming that a high degree of browning occurs. Furthermore, the data show that the major part of the colour change occurs during the first 30 min of exposure, and that during the rest of the time the changes are minimal.

As to the modelling of the colour change kinetics, various models were tested and the results showed that the models that best fitted the experimental data were the logistic, the modified Maskan and exponential raise. In these three models, the statistical analysis made proves that the fits are very adequate to the experimental sets of data.

## References

Al-Harahsheh, M., A. H. Al-Muhtaseb, and T. R. A. Magee. 2009. Microwave drying kinetics of tomato pomace: Effect of osmotic dehydration. *Chemical Engineering and Processing*, 48(1): 524-531.

Ávila, I. M. L. B., and C. L. M. Silva. 1999. Modelling kinetics of thermal degradation of colour in peach puree. *Journal of Food Engineering*, 39(2): 161-166.

Baik, O. D., and G. S. Mittal. 2003. Kinetics of tofu color changes during deep-fat frying. *LWT – Food science and Technology*, 36(1): 43-48.

Broyart, B., G. Trystram, and A. Duquenoy. 1998. Predicting colour kinetics during cracker baking. *Journal of Food Engineering*, 35(3): 351-368.

Chen, C. R. and H. S. Ramaswamy. 2002. Color and Texture Change Kinetics in Ripening Bananas. *LWT – Food Science and Technology*, 35(5): 415-419.

Chua, K. J., A. S. Mujumdar, M. N. A. Hawlader, and S. K. Chou, and J. C. Ho. 2001. Batch drying of banana pieces – effect of stepwise change in drying air temperature on drying kinetics and product colour. *Food Research International*, 34(8): 721-731.

Chutintrasri, B., and A. Noomhorm. 2007. Color degradation kinetics of pineapple puree during thermal processing. *LWT – Food science and Technology*, 40(2): 300-306.

Corzo, O., N. Bracho, and J. Marjal. 2006. Color change kinetics of sardine sheets during vacuum pulse osmotic dehydration. *Journal of Food Engineering*, 75(1): 21-26.

Cruz, R. M. S., Vieira, M. C., and C. L. M. Silva. 2007. Modelling kinetics of watercress (*Nasturtium officinale*) colour changes due to heat and thermosonication treatments. *Innovative Food Science and Emerging Technologies*, 8(2): 244-252.

Demir, A. D., J. M. F. Celayeta, K. Cronin, and K. Abodayeh. 2002. Modelling of the kinetics of colour change in hazelnuts during air roasting. *Journal of Food Engineering*, 55(4): 283-292.

Iglesias, I., G. Echeverría, and M. L. Lopez. 2012. Fruit color development, anthocyanin content, standard quality, volatile compound emissions and consumer acceptability of several 'Fuji' apple strains. *Scientia Horticulturae*, 137(1): 138-147.

Ilo, S. and E. Berghofer. 1999. Kinetics of colour changes during extrusion cooking of maize grits. *Journal of Food Engineering*, 39(1): 73-80.

Koca, N., H. S. Burdurlu, and F. Karadeniz. 2007. Kinetics of colour changes in dehydrated carrots. *Journal of Food Engineering*, 78(2): 449-455.

Kumar, A. J., R. R. B. Singh, A. A. Patel, and G. R. Patil. 2006. Kinetics of colour and texture changes in *Gulabjamun* balls during deep-fat frying. *LWT – Food science and Technology*, 39(7): 827-833.

Lau, M. H., J. Tang, and B. G. Swanson. 2000. Kinetics of textural and color changes in green asparagus during thermal treatments. *Journal of Food Engineering*, 45(4): 231-236.

Lee, J. H. and H. J. Kim. 2009. Vacuum drying kinetics of Asian white radish (*Raphanus sativus* L.) slices. *LWT - Food Science and Technology*, 42(1): 180-186.

Maskan, M. 2001. Kinetics of colour change of kiwifruits during hot air and microwave drying. *Journal of Food Engineering*, 48(2): 169-175.

Maskan, M. 2006. Production of pomegranate (*Punica granatum* L.) juice concentrate by various heating methods: colour degradation and kinetics. *Journal of Food Engineering*, 72(3): 218-224.

Nisha, P., R. S. Singhal, and A. B. Pandit. 2004. A study on the degradation kinetics of visual green colour in spinach (*Spinacea oleracea* L.) and the effect of salt therein. *Journal of Food Engineering*, 64(1): 135-142.

Nordey, T., M. Léchaudel, M. Génard, and J. Joas. 2014. Spatial and temporal variations in mango colour, acidity, and sweetness in relation to temperature and ethylene gradients within the fruit. *Journal of Plant Physiology*, 171(17): 1555-1563.

Nuncio-Jáuregui, N., A. Calín-Sánchez, A. Carbonell-Barrachina, and F. Hernández. 2014. Changes in quality parameters, proline, antioxidant activity and color of pomegranate (*Punica granatum* L.) as affected by fruit position within tree, cultivar and ripening stage. *Scientia Horticulturae*, 165(22): 181-189.

Ochoa, M. R., A. G. Kesseler, A. De Michelis, A. Mugridge, and A. R. Chaves. 2001. kinetics of colour change of raspberry, sweet (*Prunus avium*) and sour (*Prunus cerasus*) cherries preserves packed in glass containers: light and room temperature effects. *Journal of Food Engineering*, 49(1): 55-62.

Quevedo, R., O. Diaz, A. Caqueo, B. Ronceros, and J. M. Aguilera. 2009. Quantification of enzymatic browning kinetics in pear slices using non-homogeneous L* color information from digital images. *LWT – Food science and Technology*, 42(8): 1367-1373.

Roberts J. S., D. R. Kidd, and O. Padilla-Zakour. 2008. Drying kinetics of grape seeds. *Journal of Food Engineering*, 89(4): 460-465.

Suh, H. J., D. O. Noh, C. S. Kang, J. M. Kim, and S. W. Lee. 2003. Thermal kinetics of color degradation of mulberry fruit extract. *Nahrung*, 47(2): 132-135.

Topuz, A. 2008. A novel approach for color degradation kinetics of paprika as a function of water activity. *LWT – Food science and Technology*, 41(9): 1672-1677.

Tripathy, P. P., and S. Kumar. 2009. A methodology for determination of temperature dependent mass transfer coefficients from drying kinetics: Application to solar drying. *Journal of Food Engineering*, 90(2): 212-218.

Vega-Gálvez A., A. Andrés , E. Gonzalez, E. Notte-Cuello, M. Chacana, and R. Lemus-Mondaca. 2009. Mathematical modelling on the drying process of yellow squat lobster (*Cervimunida jhoni*) fishery waste for animal feed. *Animal Feed Science and Technology*, 151(3-4): 268-279.